frontiers | Frontiers in Earth Science

TYPE Original Research
PUBLISHED 18 January 2023
DOI 10.3389/feart.2022.1018325

Check for updates

OPEN ACCESS

EDITED BY
Lihua Zuo,
Texas A&M University Kingsville,
United States

REVIEWED BY
Jiliang Wang,
Institute of Deep-Sea Science and Engineering (CAS), China
Qian-Zhi Zhou,
Sun Yat-sen University, China

*CORRESPONDENCE
Bin Zhao,
zbin_a@mail.cgs.gov.cn

SPECIALTY SECTION
This article was submitted to Marine Geoscience,
a section of the journal
Frontiers in Earth Science

RECEIVED 13 August 2022
ACCEPTED 31 October 2022
PUBLISHED 18 January 2023

CITATION
Wang X, Liu S, Zhao B, Yao Y, Wu G, Xie R, Fu Y and Ning Z (2023), Quantitative analysis of the risk of hydrogen sulfide release from gas hydrates.
Front. Earth Sci. 10:1018325.
doi: 10.3389/feart.2022.1018325

Quantitative analysis of the risk of hydrogen sulfide release from gas hydrates

Xianqing Wang[1,2,3], Siqing Liu[3], Bin Zhao[3,4]*, Yanfu Yao[1,2,3], Gang Wu[1,2,3], Rui Xie[1,2,3], Yutong Fu[1,2,3] and Zijie Ning[3]

[1]Sanya Institute of South China Sea Geology, Guangzhou Marine Geological Survey, Sanya, China, [2]Academy of South China Sea Geological Science, China Geological Survey, Sanya, China, [3]Guangzhou Marine Geological Survey, Guangzhou, China, [4]Southern Marine Science and Engineering Guangdong Laboratory, Guangzhou, China

The role that H_2S plays in the global sulfur cycle has been studied extensively in recent years. This paper focuses on the influence of H_2S released from gas hydrates on sulfur cycle and establishes a one-dimensional mathematical model to calculate the amount of H_2S released from the dissociation of gas hydrates present in multiple layers in the Qiongdongnan Basin China. The results show that the sulfate and methane transition zone that covers an area of about 100 km^2in the Qiongdongnan Basin contains 2.3×10^{12} g of pyrite, which requires 4.06×10^{11} mol of H_2S for its formation. The H_2S released from the dissociation of gas hydrates is 5.4×10^{11} mol, which is about 1.3 times that needed for the formation of pyrite. Therefore, the H_2S released from the gas hydrates is an important source of H_2S for the formation of pyrite in the sulfate-methane transition zone of Qiongdongnan Basin. According to the flux of H_2S and the partial pressure of O_2 (P_{O2}) in the atmosphere, the critical value of the balance between the flux of H_2S and P_{O2} turns out to be 0.13 mol kg^{-1}·bar^{-1}. Furthermore, considering the effect of global sea-level changes, three risk modes are identified to categorize the amount of H_2S released from the dissociation of gas hydrate into the atmosphere. We classify the periods from 5–12 Ma BP, 25–29 Ma BP, 47–52 Ma, and 57–61 Ma BP into the high-risk mode. Furthermore, the results show that a part of the H_2S released from the gas hydrate dissociation is oxidized by the Fe (III) oxide metal, with much of the metal ions being released into the pore water. Another part of the H_2S is re-oxidized by the O_2 in the ocean, with much of SO_4^{2-} released into the seawater. Therefore, the process also provides metal ions and SO_4^{2-} to pore water or seawater when the H_2S released from gas hydrate diffuses from the bottom. This paper provides new insights into the source of H_2S in the ocean and shows that the H_2S contained in gas hydrates plays an important role in the global sulfur cycle.

KEYWORDS

sulfur cycle, hydrogen sulfide, pyrite formation, anaerobic oxidation, methane

1 Introduction

Pyrites are the most important sulfur sinks and are widely distributed in marine sediments (Lin et al., 2017). They have a significant influence on the sulfur cycle and have resulted in a series of studies involving major scientific issues, such as the evolution of oxygen and the origin of life (Butler et al., 2004; Chen et al., 2006; Formolo and Lyons 2013; Akhoudas et al., 2018). Therefore, many scholars have carried out detailed research on their cause and isotope composition (Hu et al., 2012; Pan et al., 2018). Two pyrite formation pathways have been proposed. One pathway is the polysulfide one:

$$FeS_{(s)} \rightarrow FeS_{(aq)} + S^{2-}_{n\,(aq)} = FeS_{2\,(aq)} + S^{2-}_{n-1}\,(aq) \qquad (1)$$

The other is the H_2S pathway, initially observed as the reaction of pyrrhotite ($Fe_{1-x}S$) with $H_2S_{(aq)}$:

$$FeS_{(s)} \rightarrow FeS_{(aq)} + H_2S_{(aq)} = FeS_{2\,(S)} + H_2\,(g) \qquad (2)$$

There have been many studies related to the formation of pyrite, right from the identification of the macroscopic sedimentary environment to the microscopic microbial culture, and are mainly focused on the redox state of the sedimentary environment and the global C-S-Fe cycle (Peckmann and Thiel 2004; Kraal et al., 2009; Lin et al., 2016). In recent years, the influence of the local depositional environment on the formation of pyrite and its isotopes has received increasing attention, and the idea of using pyrite sulfur isotopes to trace the evolution of depositional environment (such as sea-level changes) has been put forward (Wang et al., 2018a), especially in shallow seas (Peckmann et al., 2001; Lim et al., 2011; Sima et al., 2011). During OSR and SO_4^{2-}-AOM processes, higher HS- concentrations are produced in the pore water and HS- reacts with Fe^{2+} in pore water or sediment to form pyrite. During this process, metal oxides are gradually converted into FeS and finally into pyrite under the action of excessive hydrogen sulfide. Therefore, studying the source of hydrogen sulfide has important scientific significance to understand the change of depositional environments. However, the speciation of H_2S in seawater is complex, with the species most often described in terms of free sulfide (H_2S+ HS^-+ S^{2-}). Furthermore, questions remain regarding the role that H_2S plays in the global sulfur cycle, particularly with respect to its presence in the remote oceanic atmosphere and possible transfer across the air/sea interface. Previous studies have found that the main source of hydrogen sulfide for the formation of pyrite in marine sediments is from the anaerobic oxidation of methane (AOM) and organic sulfur reduction (OSR) (Xie et al., 2019; Wei et al., 2020). The production of hydrogen sulfide also occurs in hydrothermal systems due to geochemical processes (Yao and Millero, 1996). Huene and Pecher, (1999) summarized the H_2S concentrations found in a large number of hydrothermal fluids at various locations in the Pacific and Atlantic oceans, whereas the concentrations ranged from 1.1 to 110 mmol kg^{-1} (Von et al., 1995). However, previous studies have focused more on the mechanism of the formation of hydrogen sulfide and the source of hydrogen sulfide from volcanic eruptions, hydrothermal flux, or from the AOM and OSR (Radford- Knwry and Cutter, 1994, Shen et al., 2008; Wu et al., 2018). Only a handful of studies have focused on hydrogen sulfide contained in hydrates. At present, H_2S has been observed in gas hydrates using Raman spectroscopy at the Hydrate Ridge (Hester et al., 2007), the Nigerian Margin (Chazallon et al., 2007), and the South China Sea (Fang et al., 2019). In marine sediments, there are huge reserves of gas hydrates, which are widely distributed. There are also huge reserves of H_2S in gas hydrates, which are universally present across the Earth. Moreover, H_2S released from gas hydrates has an important influence on the environment. Considering the huge reserves of

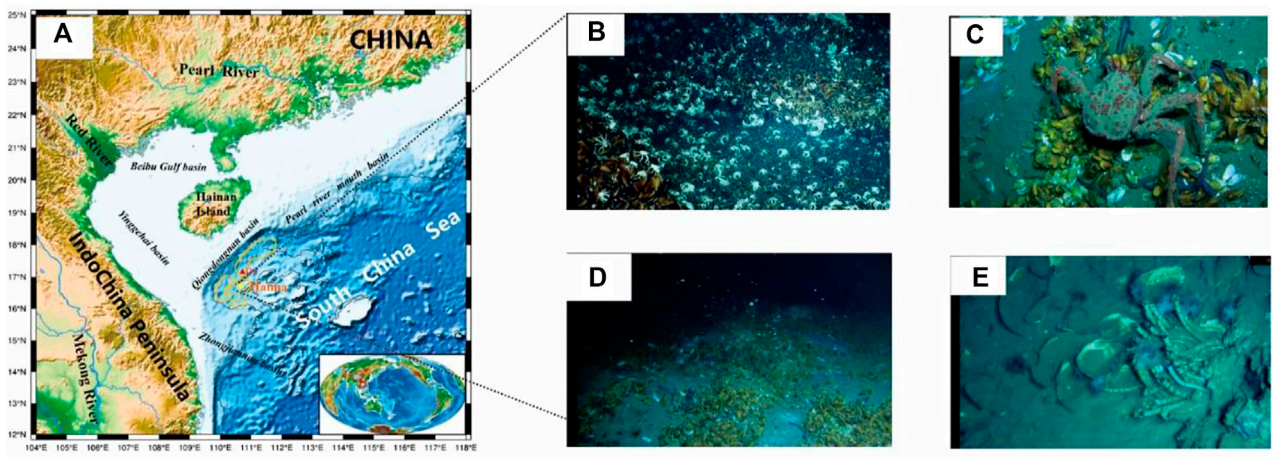

FIGURE 1
The methane seep area was observed in Qiongdongnan Basin. [**(A)**: Study Area, **(B–E)**: Biological status of methane leakage area].

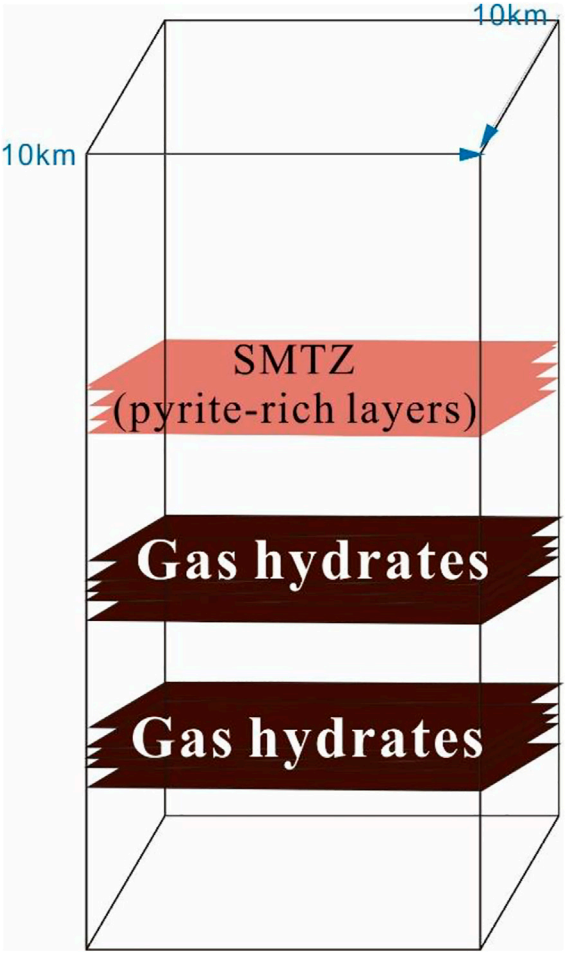

FIGURE 2
The mode distribution of gas hydrate and sulfate methane transition zone.

gas hydrates, the amount of H_2S contained in gas hydrates is also huge. Furthermore, when gas hydrates dissociate, much of the H_2S released from the gas hydrates also affect the environment, the sulfur cycle in the ocean, and the local ecosystem (Kastner et al., 1998). Therefore, it is important to study the role that gas hydrates play in pyrite formation.

2 Geological setting

Qiongdongnan Basin is located in the western part of the northern continental slope of the South China Sea (Figure 1). The northern part of the basin is bound by the Hainan Island, while the west is adjacent to Indochina. Additionally, the east is close to the Pearl River Mouth Basin. The Qiongdongnan Basin covers more than 80,000 km^2, and approximately 60% of the basin has a water depth of more than 300 m (Wang et al., 2015). The seafloor water temperature at the Qiongdongnan Basin is 2°C–3°C, and the mean geothermal gradient is approximately 40°C/km. However, due to the common gas-bearing fluid activity in the Qiongdongnan Basin, the geothermal gradient in the study area is relatively much higher (Yuan et al., 2009). Oil and gas have been discovered in multiple reservoirs in different structural tectonic belts in the Qiongdongnan Basin (QDNB) (Zhang et al., 2014; Wang et al., 2015; W. Zhang et al., 2015; Zhang et al., 2016; Qin et al., 2019). The sediments deposited during the Pliocene and Quaternary possess favorable conditions for hosting biogenic gases, and these were commonly encountered in the strata shallower than 2,300 m during gas logging. In addition, the coal-measure source rocks deposited in the Oligocene are in the thermal evolution stage of mature-to-high-mature, with favorable conditions for thermogenic gas generation (Huang et al., 2015; Huang et al., 2017). Overpressure was common during the formation of QDNB when the rapidly filling sediments deposited in the Cenozoic became deeply buried under compaction (Shi et al., 2019; Wang et al., 2020). The mud diapirs and gas chimneys caused by overpressure are widely distributed in the deep water, providing an important vertical migration pathway for hydrocarbons and for the formation and accumulation of natural gas hydrates (Zhang et al., 2016; Wang et al., 2020). Furthermore, there is a large concentration of bivalve shells in the methane seep area (Figures 1B–E), indicating that the methane flux is higher. Meanwhile, multiple layers of gas hydrate are also found in the study area (Liang et al., 2019) (Figure 2).

3 Methods

In the current study, we used mass conversation equations to calculate the amount of H_2S in the sink and how much H_2S is released from the sink.

The total mass of H_2S at any given time can be described as:

$$\frac{d}{dt}H_2S = H_2S_{RG} + H_2S_{RA} + H_2SS_{RO} + H_2S_{PH} - H_2S_{FP} - H_2S_{RM} - H_2S_O \tag{3}$$

where H_2S_{RG} denotes the H_2S released from gas hydrate dissociation, H_2S_{RA} denotes the H_2S produced from AOM, H_2S_{R0} denotes the H_2S_{RO} produced by OSR, H_2S denotes the H_2S released from hydrothermal sources, H_2S_{FP} denotes the H_2S that reacts with the metal ions to form pyrite, H_2S_{RM} denotes the H_2S that is oxidized by the Fe (III) oxides, and H_2S_O denotes the H_2S that is oxidized by oxygen. In the study area, there is no volcanic and hydrothermal activity. Therefore, in the current paper, the H_2S_{PH} is assumed to be zero.

In the present study, the percentage of H_2S in gas hydrates was confirmed by the relative peak intensities of H_2S to CH_4. in

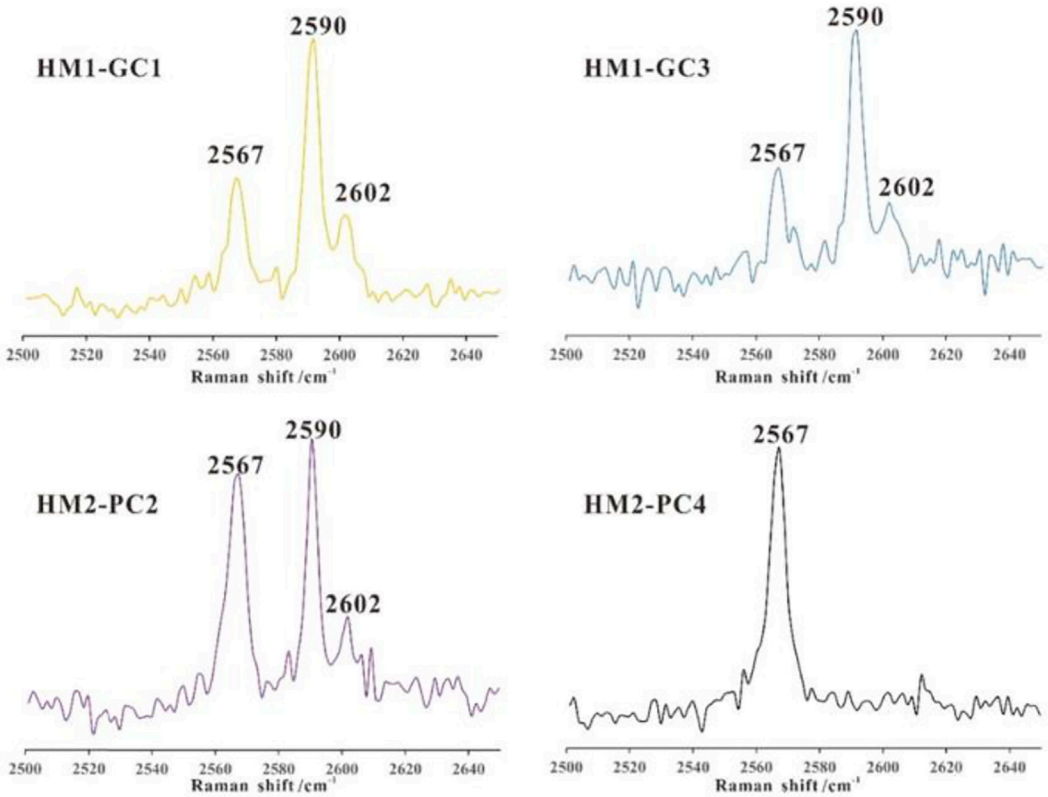

FIGURE 3
The concentration of H_2S in gas hydrate at Qiongdongnan basin (Referend from huang et al., 2017).

Spectroscopy. Moreover, their Raman quantification factor ratios were calibrated using the crystal established absolute cage occupancies of a pure H_2S sample (Figure 3) (Qin and Kuhs 2013), which is similar to the procedures described in (Qin and Kuhs, 2013) for CH_4 hydrate.

The percentage values of the partial pressure of atmospheric oxygen (P_{O2}) are determined by Liu et al. (2021) and the present value of P_{O2} is 212.28 mbar. The geological time of P_{O2} is determined by multiplying the fraction of P_{O2} with 212.28 mbar.

4 Results and discussion

4.1 Influence of the H_2S released from gas hydrates on the formation of pyrite

In marine sediments, the formation of H_2S occurs in a variety of settings. The production of H_2S in the pore water of sediments and the water column of stagnant basins is due to the anaerobic oxidation of methane (Yang et al., 2007). Submarine hydrothermal emissions are also a possible source of H_2S to the ocean. However, previous studies have shown that H_2S released from submarine hydrothermal emissions are not easily transferred into the atmosphere and shallow sediments (Yao and Milero., 1996). Therefore, the organic sulfur reduction (OSR) and anaerobic oxidation of methane (AOM) are the main sources of H_2S for the formation of pyrite (Commeau et al., 1987; Egger et al., 2015; Lin et al., 2015; Xie et al., 2019; Wu 2020; Wu, 2020; Wu, Xie, et al., 2020). However, the question remains as to how to evaluate the quantity of H_2S involved in the process of the formation of pyrites. As we all know, the AOM is widely present in the seepage area of gas hydrates (Wang et al., 2018b). Pyrites are also concentrated in sulfate and methane transition zone. During the process of AOM, the methane diffused from the bottom reacts with the sulfate from the overlying water at the sulfate-methane transition zone (SMTZ). The specific process is as follows:

$$CH_4 + SO_4^{2-} \rightarrow HS^- + HCO_3^- + H_2O \quad (4)$$

From Eq. 4, assuming the same reaction rate conditions, when 1 mol of methane is reduced by the sulfate, 1 mol of HS^- is produced at the same time. However, during the process of pyrite formation, 2 mol HS^- is needed to form 1 mol of pyrite (Peckmann et al., 2001; Canet et al., 2006; Lin et al., 2017). The specific reactions are as follows:

$$Fe^{2+} + HS^- \rightarrow FeS + H^+ \quad (5)$$

$$FeS + H_2S \rightarrow FeS_2 + H_2 \quad (6)$$

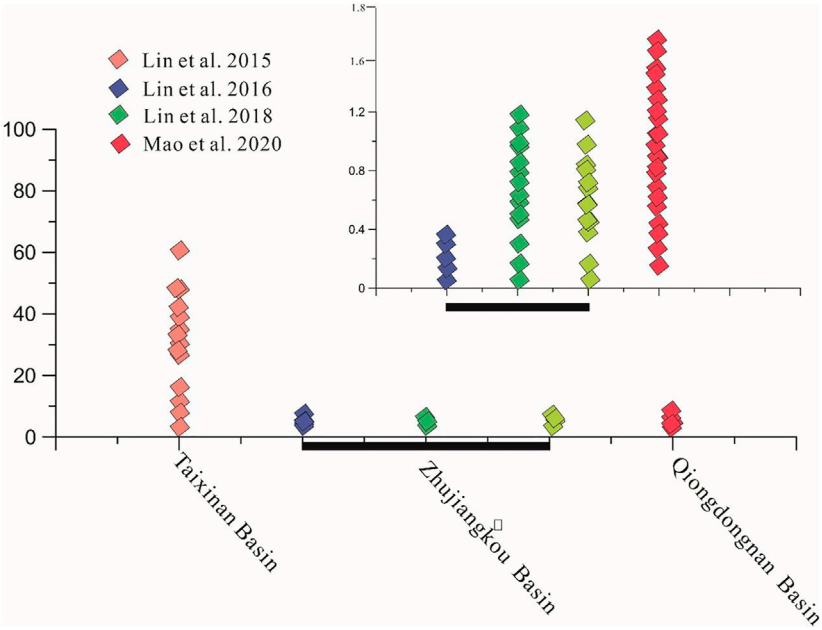

FIGURE 4
Content of pyrite at sulfate and methane transition zone in different sediments basin.

Moreover, 1 mol of hydrogen sulfide is provided by the AOM process, and another 1 mol is provided by another unknown mechanism. The presence of H_2S in the gas hydrates provides an explanation (Qin et al., 2020). Of course, organic sulfur reduction (OSR) also provides part of the missing H_2S. The specific reaction is as follows:

$$2CH_2O + SO_4^{2-} \rightarrow 2HCO_3^- + H_2S \tag{7}$$

However, OSR often takes place in the open environment and shallower sediments as compared to AOM (Xie et al., 2019). Therefore, the hydrogen sulfide produced by the OSR is always diffused upwards under the influence of pressure gradient. Due to this reason, it is difficult for it to be diffused downwards.

In the study area, the SMTZ is mainly distributed at 6–9 mbsf in the Taixinan Basin and the content of pyrite in the sediments is about 1.16%–1.03% at Taixinan Basin (Wu et al., 2019; Wei, et al., 2020). Previous studies have shown that the content of pyrite at the Zhujiangkou Basin, where the SMTZ is present at 5–7 mbsf, is about 2.5%–2.6% (Liu et al., 2016). In the Qiongdongnan Basin, the content of pyrite lies within the range of 1%–3%, and the SMTZ is distributed at about 2–3.9 mbsf. Furthermore, the SMTZ is also very close to the water-sediment seafloor, indicating that the methane flux is high in the Qiongdongnan area (Miao et al., 2021). During the GMGS5 voyages, the methane seep area was found, which covered an area of about 100 km^2 in the Qiongdongnan Basin (Figure 1). In this area, there is a rich concentration of gas hydrates and pyrites in the sediments. Based on the above analysis, the amount of pyrite in the SMTZ deposits in the methane seep area in the Qiongdongnan Basin can be calculated using the following equation

$$Quantity_{pyrite} = Depth_{SMTZ} \times S_{methane\ seep\ area} \times Q_{sediment\ density} \times C_{the\ pyrite\ percent\ of\ sediments} \tag{8}$$

$$Mole\ H_2S = \frac{Quantity_{pyrite}}{m} \times 2 \tag{9}$$

In this paper, m represents the relative molecular weight of pyrite. The depth of the SMTZ is 1.9 m, whereas the cover area is 100 km^2. Moreover, Q ranges from 1.64 to 1.9 g/cm^3 (Zhang et al., 2015; Liang et al., 2019). We selected a sediment density of 1.8 g/cm^3 and a pyrite percentage in the sediment of 2% in the Qiongdongnan Basin (Figure 4) (Mao et al., 2021; A. Haggerty 1991; Lim et al., 2011). The calculated quantity of pyrite is 6.9×10^{12} g. Therefore, the H_2S needed to form pyrite is 4.06×10^{11} mol. The same methods can be applied to calculate the quantity of H_2S released from the gas hydrates (see Eq. 10).

$$Quantity_{gas\ hydrate} = Depth_{gas} \times S \times Q_{sediment\ density} \times Saturation\ of\ gas\ hydrate \tag{10}$$

In this equation, the $Depth_{gas\ hydrate}$ has been confirmed to be deposited at the three sediments sections (18.55–40.42 mbsf, 43.42 to 56.12 mbsf, and 58.6 to 98.42 mbsf) and was based on coring and sampling results

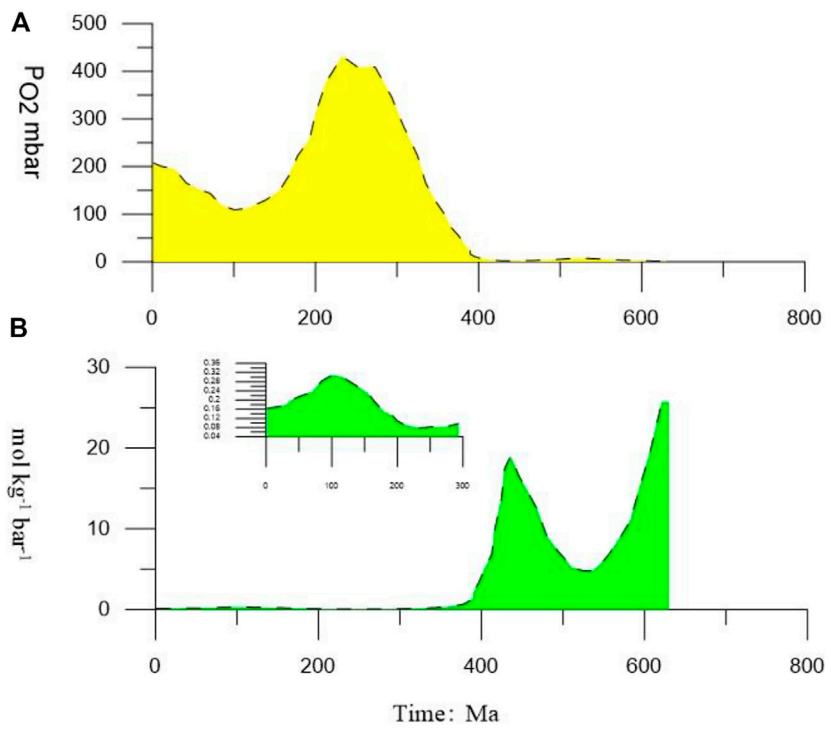

FIGURE 5
(A) Variation in the value of P_{O2} from present to 600 Ma BP. **(B)** Critical values changes from present to 600 Ma BP under the H_2S released from the complete dissociation of the first layer of gas hydrate. Moreover, from the present to 400 Ma, the H_2S released from the complete dissociation of the first layer of gas hydrate hardly moves into the atmosphere.

and pilot hole LWD anomalies, which showed a high resistivity, low density, high gamma-ray values, and elevated acoustic velocity (Liang et al., 2019) Herein, the first Depth $_{gas}$ is 21.87 m, the second Depth $_{gas}$ is 13 m, and the saturation of gas hydrate is 31%. The quantity of gas hydrate in the first layer is 1.22×10^{15} g. The percentage of H_2S in the gas hydrate ranges from 1% to 2%, and, therefore, the quantity of H_2S in the gas hydrate of the first layer is 1.83×10^{13} g. The moles of H_2S released from the dissociation of gas hydrates in the first layer can be calculated using the following equation:

$$Mole\,H_2S = \frac{Quantity_{H2S}}{d} \tag{11}$$

According to this analysis, the released quantity of H_2S is 5.4×10^{11} mol. The H_2S released from the gas hydrate is about 1.3 times the H_2S needed for the formation of pyrite. The calculation results show that the H_2S released from the dissociation of gas hydrates may be the source of H_2S required to form pyrites. What is more, a greater volume and continual release of H_2S from the gas hydrate could cause the H_2S to seep into the water and even into the atmosphere. If so, it is still not clear what its biological and chemical consequences could be.

4.2 Evaluating the concentration of H_2S released from gas hydrates into the ocean and atmosphere

In general, H_2S can be depleted in seawater *via* oxidation. Recognized loss processes include photochemical oxidation, reaction with dissolved oxygen (Millero et al., 1987), After hydrogen sulfide ($HS=H_2S+HS^{-}+S^{2-}$) is produced, it mainly participates in three types of reaction processes: 1) It gradually diffuses to the seabed and enters the bottom seawater body or oxidizes during the diffusion process. The oxidants in this process include oxygen, Iron oxides and manganese-containing oxides, products include elemental sulfur (S_0), complex sulfides (e.g., $S_2O_3^{2-}$) and sulfates; 2) Combine with organic matter to form organic sulfur; (three is also the most important reaction process, that is, it combines with iron-bearing minerals to form iron-bearing polysulfides and monosulfides and finally converts to pyrite. This is also the main formation mechanism of pyrite in marine sediments. In addition, a large number of laboratory studies have shown that pyrite can also be formed directly without the transformation of iron polysulfides. However, it is not all HS required for pyrite formation comes from SO_4^{2-}-AOM. (Kelly and Kadish, 1982). However, in marine anoxic sediments, the concentration of oxygen and is low. Yao and Millero, 1996 found that elemental sulfur was the dominant

product (95–100%) produced by the oxidation of H_2S by hydrous Fe(III) oxides. In fact, elemental sulfur is seldom found in the marine sediments in the Qiongdongnan Basin. Therefore, in anoxic sediments, the H_2S released from gas hydrates cannot be easily consumed, except in the process of forming pyrite. Nanomolar levels (0.1–2 nM) of H_2S have been found in the surface waters of the oceans (Cutter and Oatts, 1987; Iii and Tsamakis, 1989). However, the mechanism of the production and maintenance of hydrogen sulfide in surface seawater remains unclear. As is discussed in Section 4.1, if the second layer of gas hydrate dissociation results in the release of hydrogen sulfide into seawater, the main controlling factor for the release of hydrogen sulfide into the atmosphere is oxygen. In fact, in anoxic basins, mildly sulfidic deep waters are separated from the atmosphere by an oxygenated surface layer, at the base of which is a sulfide chemocline through which O_2 concentrations fall to zero. Kump et al. (2005) found that a significant buildup of H_2S in the deep sea could have led to toxic emissions of H_2S into the atmosphere, methane accumulation, and global warming Kump et al. (2005). The question is how to evaluate the seepage of H_2S into the water or atmosphere, and that the fundamental characteristic affecting the supply of H_2S into the water or atmosphere is the supply of O_2, whose transport through the surface layer must exceed the upwelling and diffusive flux of the reductant (H_2S) from below. The flux of O_2 must be at least two times the concentration of H_2S given the stoichiometry of the following reaction:

$$H_2S + 2O_2 \rightarrow SO_4^{-2} + 2H^- \tag{12}$$

The fundamental characteristic of a stable chemocline is that the supply of O_2 from the atmosphere across the air-sea interface and its transport through the surface layer must exceed the upwelling and diffusive flux of the reductant (H_2S) from below. Kump et al. (2005) treated the exchange of gases, including O_2, between the atmosphere and ocean by using a piston-velocity formulation, whereby the flux of gases occurs at a rate (in this case, F_{O2}) that is proportional to the contrast in gas concentrations between the atmosphere and surface ocean with the proportionality constant being the piston velocity (k):

$$F_{O2} = \rho_{oce} \cdot k \cdot K_H \ (P_{O2atm} - P_{O2oce}) \tag{13}$$

The supply of H_2S from below by upwelling (F_{H2S}) can be written as

$$F_{H2S} = \rho_{oce} \cdot u \cdot [H_2S]deep \tag{14}$$

where u is the upwelling rate (four in $m \cdot yr^{-1}$), $[H_2S]_{deep}$ is the concentration of H_2S in deep waters (in $mol \cdot kg^{-1}$), ρ_{oce} is the density of seawater (1,002 kg/m^3), and K_H is the Henry's law constant for O_2 (for warm surface waters, K_H is 10^{-3} $mol\ kg^{-1} \cdot bar^{-1}$).

The critical conditions for the balance of O_2 and H_2S must conform to the following equations:

$$F_{O2} = 2F_{H2S} \tag{15}$$

$$\rho_{oce} \cdot k \cdot K_H \ (P_{O2atm} - P_{O2oce}) = 2\,\rho_{oce} \cdot u \cdot [H_2S]deep \tag{16}$$

Given these values, and setting the surface water O_2 partial pressure (P_{O2oce}) to zero, the P_{O2oce} critical ratio of H_2S in the deep to atmospheric O_2, above which the steady-state surface-water O_2 concentration is zero, is given by Eq. 17.

$$\left(\frac{H2S_{deep}}{P_{O2,\,atm}}\right) = \frac{k \cdot KH}{2u} = \frac{1000m\,yr - 1 \times 10 - 3\,mol\,kg - 1\,bar - 1}{2 \times 4\,m\,yr - 1}$$

$$\approx 0.13\,\frac{mol}{kg\,bar} \tag{17}$$

In the study area, the dissociation of the first gas hydrate layer would cause the H_2S to reach 0.135 $mol\ kg^{-1}$, and, at present, $P_{O2\ atm}$ is 212.28 mbar. Hence, $\frac{H2S_{deep}}{P_{O2,\,atm}}$ present $= \frac{0.135 mol \cdot kg-1}{212.28 \times 10-3 bar} \approx 0.64\ \frac{mol}{kg\,bar}$. 0.64 $mol\ kg^{-1} \cdot bar^{-1}$ (Figure 5) is greater than the critical value of 0.13 $mol\ kg^{-1} \cdot bar^{-1}$. Due to this reason, the dissociation of the gas hydrate in the first layer would cause a subsequent release of H_2S that could easily enter the atmosphere in the present condition of P_{O2}. However, during geological time, P_{O2} often changes with time, so at different geological times, the critical values would vary (Table 1). In this paper, we calculated the various critical values from the present to 600 Ma. Our results show that, from 0 to 200 Ma, the H_2S easily seeped into the atmosphere through the dissociation of gas hydrate in the first layer. From 200 to 300 Ma, the calculated H_2S_{deep}/P_{O2} values are lower than the standard values. Therefore, it would have been difficult for the H_2S to seep into the atmosphere if the temperature and pressure changed during this geological time.

4.3 Evaluation of the influence of gas hydrate dissociation on H_2S release through geological time

Gas hydrates are sensitive to temperature and pressure (Wan et al., 2022). When these factors change, the gas hydrates can dissociate. Previous studies have shown that gas hydrates are sensitive to sea-level changes (Chown et al., 2000; Blendinger 2004; Bangs and Nathan, 2005; Jang-Jun et al., 2011). A decrease in sea level will cause a corresponding change in the pressure. These pressure changes can gradually cause the gas hydrates to dissociate. In fact, in the sediments with normal methane seepage, it is difficult for the hydrogen sulfide produced by AOM to reach the water, but the existence of methane-hydrogen sulfide hydrate makes large-scale hydrate decomposition that may lead to massive hydrogen sulfide release. At this time, it is particularly important to evaluate the conditions under which the hydrogen sulfide gas reaches the water body. In this study, we assume that the gas hydrate in the first layer is more susceptible to changes in the sea-level, resulting in a

TABLE 1 The partial pressure of atmospheric oxygen level at different geological period.

Geological time	Partial pressure of atmospheric oxygen level (%)	P_{O2mbar}
1.37	99.13	207.22
11.45	99.13	200.10
27.32	96.56	194.35
41.66	93.79	165.08
56.01	79.66	152.14
70.35	73.42	143.95
84.85	69.47	118.76
100.57	57.31	109.13
116.44	52.66	112.36
137.96	54.22	128.86
155.21	62.18	147.77
166.81	71.31	179.12
178.25	86.44	222.88
192.60	107.56	256.35
199.92	123.71	310.73
212.74	149.95	376.64
232.89	181.76	431.94
251.66	208.44	408.67
273.18	197.21	408.67
293.32	197.21	346.11
307.67	167.03	285.54
325.07	137.80	222.88
335.14	107.56	165.08
345.21	79.66	132.28
358.03	63.84	100.58
365.20	48.54	74.28
375.28	35.85	55.02
379.70	26.55	45.39
383.98	21.90	32.65
389.77	15.76	24.75
389.77	11.95	16.41
394.05	7.92	11.81
398.32	5.70	8.98
404.12	4.33	6.63
412.67	3.20	4.90
415.57	2.36	3.52
424.27	1.70	2.47
428.54	1.19	1.93
435.71	0.93	1.78
445.78	0.86	2.04
467.46	0.98	2.68
480.27	1.29	3.72
493.25	1.80	4.63
501.95	2.24	5.33
510.49	2.57	6.46
524.99	3.12	7.01
536.44	3.38	7.01
546.51	3.38	5.93
556.58	2.86	4.90
570.93	2.36	3.72
582.53	1.80	3.07
591.07	1.48	2.40
606.94	1.16	1.72
621.29	0.83	1.31
629.99	0.63	1.31

dissociation of the gas hydrate in the first layer. The gas hydrate in the second layer is assumed to be gradually released, causing a 20%, 40%, 60%, 80%, and 100% release of H_2S. Previous studies have shown that the H_2S released from the dissociation of gas hydrates in the first layer easily seeps into the atmosphere, except during 192–307 Ma BP. When 20% of H_2S is released from the gas hydrate in the second layer, it easily seeps into the atmosphere, except from 199 to 325 Ma. When the H_2S released by the dissociation of gas hydrates in the second layer reaches 40%, it also easily seeps into the atmosphere, except from 199 to 273 Ma (Figure 6). When the H_2S released by the dissociation of gas hydrates in the second layer reaches 60%, it easily seeps into the atmosphere, except from 212 to 293 Ma. When the H_2S released by the dissociation of gas hydrates in the second layer reaches 80%, it easily seeps into the atmosphere, except from 212 to 273 Ma. When the H_2S released by the dissociation of gas hydrates in the second layer reaches 100%, it easily seeps into the atmosphere, except from 232 to 273 Ma. For more precise estimates of the risk of H_2S being released into the atmosphere from the dissociation of gas hydrates, we incorporated the effects of sea-level change from 100 Ma BP to today and identified three risk modes: 1) the high-risk mode indicates that the sea level decreased sharply causing large-scale gas hydrate dissociation. The P_{O2} value within this geological period is low. In this case, the H_2S released into the atmosphere is high. 2) The moderate-risk mode indicates that the sea level decreased slower than in the high-risk mode and caused partial gas hydrate dissociation. However, the P_{O2} values during geological time are at a higher level. In this case, the amount of H_2S released into the atmosphere was moderate. 3) The low-risk mode indicates that the sea level is high and the P_{O2} values during this geological period are also high. In

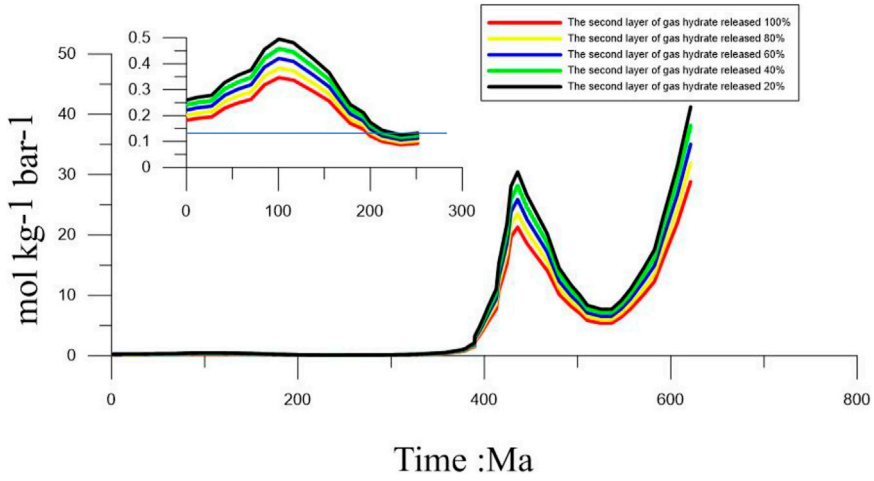

FIGURE 6
Variation in the values from 600 Ma BP under the gradual dissociation of second gas hydrate from 20% to 100%.

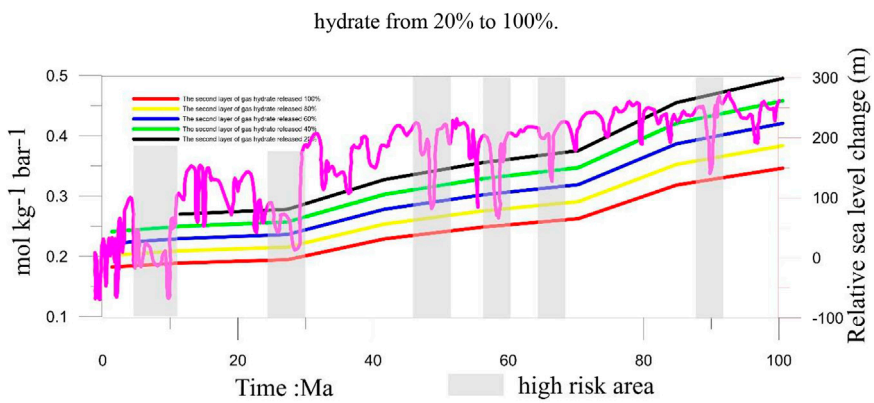

FIGURE 7
Risk ranging from present to 100 Ma BP. The purple curve represents the change in global sea level. The grey area represents the high risk of H_2S going into the atmosphere.

this case, the H_2S released from the gas hydrate would not easily seep into the atmosphere. Based on the three risk modes, we classified 5–12 Ma BP, 25–29 Ma BP, 47–52 Ma, and 57–61 Ma BP into the high-risk mode. In addition, we draw a conclusion through detailed analysis: When geological time of the P_{O2} was low and the gas hydrate's temperature and pressure changed greatly, it caused massive gas hydrate dissociation resulting in a massive amount of H_2S being released from the gas hydrates and diffusing into the pore water from the bottom. During the process, part of the H_2S released from the gas hydrate was oxidized by the Fe (III) oxide metals, and part of it was used to form pyrite. Most of the H_2S entered the ocean and even into the atmosphere. When geological time of the P_{O2} is high, the sea-level changed greatly. Meanwhile, massive H_2S was released from the gas hydrate into the pore water. This released H_2S will diffuse from the bottom. During the process, a small part of H_2S was released from the gas hydrate (being the H_2S source) to form pyrite. However, most of the H_2S will enter the ocean and get re-oxidized to become sulfate by the O_2 in the ocean. Furthermore, the H_2S released from the dissociation of the gas hydrates would be oxidized by Fe (III) oxide metals, with much of these metal ions being released into the pore water. In addition, the H_2S that was re-oxidized by the O_2 in the ocean also released much of the SO_4^{2-}. Therefore, the process also provides metal ions and SO_4^{2-} into pore water or seawater

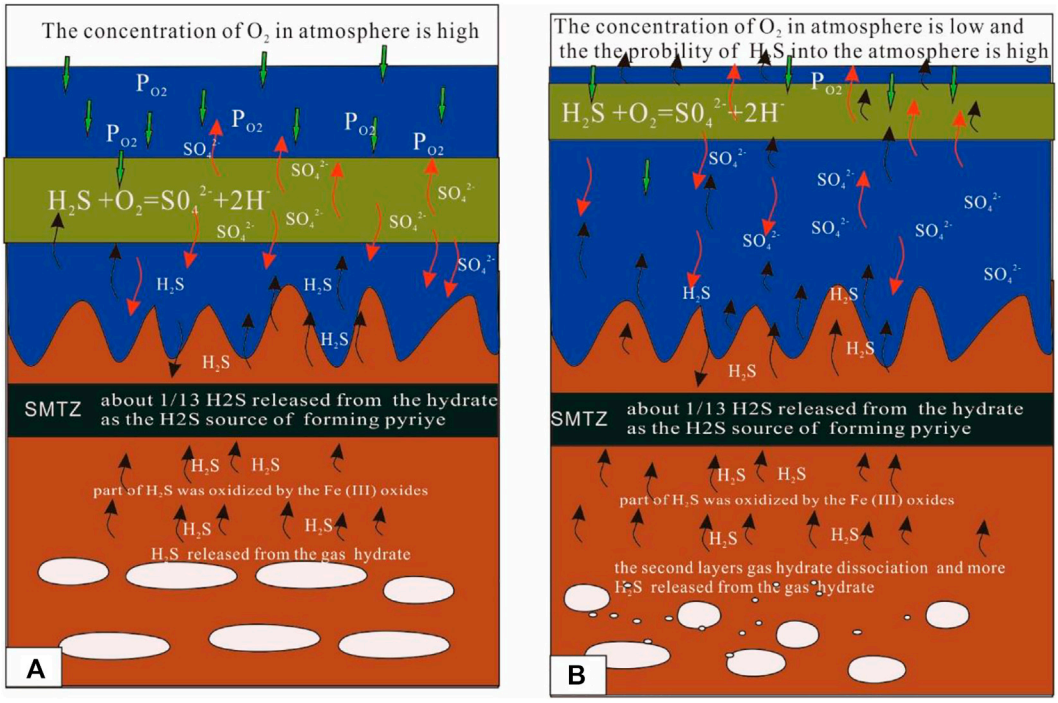

FIGURE 8
Mode of the sulfur cycle. The results show that a part of the H_2S released from the dissociation of the gas hydrate is oxidized by Fe (III) oxide metal, with much of the metal ions being released into the pore water. Another part of the H_2S is re-oxidized by the O_2 in the ocean, with much of SO_4^{2-} released into the seawater. Therefore, the process also provides metal ions and SO_4^{2-} to pore water or seawater when the H_2S released from the gas hydrate diffuses from the bottom. The difference in A and B is the level of P_{O2}. In **(A)**, the P_{O2} is high and the released hydrogen sulfide from the decomposition of hydrate finds it difficult to enter the atmosphere. In **(B)**, the P_{O2} is low and the released hydrogen sulfide from the decomposition of hydrate finds it easy to enter the atmosphere.

when the H_2S released from gas hydrate diffuses from the bottom.

5 Conclusion

It is important to evaluate how H_2S is released from gas hydrates. In this study, we established a one-dimensional mathematical model to calculate the amount of H_2S released from multiple layers of gas hydrates in the Qiongdongnan Basin. We investigated the role that H_2S released from the dissociation of gas hydrates plays on the sulfur cycle. Furthermore, we established the relationship between H_2S released from gas hydrate dissociation and the concentration of H_2S in the atmosphere. Our results show that the sulfate and methane transition zone (SMTZ) in the Qiongdongnan Basin contains 2.3×10^{12} g of pyrite, which requires 4.06×10^{11} mol of H_2S for its formation. The amount of H_2S released from the gas hydrate dissociation is 5.4×10^{11} mol, which is about 1.3 times more than that needed for the formation of pyrite. Therefore, the H_2S released from the dissociation of gas hydrates is an important source of H_2S for the formation of pyrites in the SMTZ in the Qiongdongnan Basin. Based on the flux of H_2S and the partial pressure of O_2 (P_{O2}) in the atmosphere, we calculated the critical value of the balance between the flux of H_2S and P_{O2} to be 0.13 mol $kg^{-1} \cdot bar^{-1}$. Furthermore, considering the effects of global sea-level change, we determined three risk modes to evaluate the possible seepage of H_2S from gas hydrate dissociation into the atmosphere. These are as follows: 1) the high-risk mode indicates that the sea level decreased sharply causing large-scale gas hydrate dissociation. The P_{O2} values during this geological time are low. In this situation, there was a larger amount of H_2S released into the atmosphere. 2) The moderate-risk mode indicates that the sea level decreased gradually and caused partial gas hydrate dissociation. However, the P_{O2} values at this geological time are higher. In this case, the amount of H_2S released into the atmosphere was moderate. 3) The low-risk mode indicates that the sea level is high, and the P_{O2} values at this geological time are also higher (Figure 7). Therefore, it was not easy for the H_2S released from the gas hydrate dissociation to seep into the atmosphere. Based on the three risk modes, we classified 5–12 Ma BP, 25–29 Ma BP, 47–52 Ma, and 57–61 Ma BP into the high-risk mode. Furthermore, the H_2S released from the

gas hydrate was oxidized by Fe (III) oxide metals, with much of the metal ions being released into the pore water. The H_2S that was re-oxidized by the O_2 in the ocean also released a lot of SO_4^{2-} (Figure 8). Therefore, the whole process also provides the raw materials for the process itself. This paper provides new insights into the source of H_2S found in the atmosphere and shows that the H_2S contained in gas hydrates possibly plays an important role in the global sulfur cycle.

Data availability statement

The original contributions presented in the study are included in the article/supplementary material, further inquiries can be directed to the corresponding author.

Author contributions

XW: Conceptualization, Methodology, Writing—Original Draft. SL: Data Curation. BZ: Conceptualization, Supervision, Writing—Review and Editing. YY and GW: Supervision. RX: Writing—Review and Editing. YF and ZN: Funding Acquisition, Resources, Supervision. All authors contributed to the manuscript.

Funding

The research was supported by the Project of Sanya Yazhou Bay Science and Technology City (No. SCKJ-JYRC-2022-14), GuangDong Basic and Applied Basic Research Foundation (No. 2020A1515110405), Geology Investigation Project of China Geological Survey (No. DD20221725), National Natural Science Foundation of China (No. 42106078).

Conflict of interest

The authors declare that the research was conducted in the absence of any commercial or financial relationships that could be construed as a potential conflict of interest.

Publisher's note

All claims expressed in this article are solely those of the authors and do not necessarily represent those of their affiliated organizations, or those of the publisher, the editors and the reviewers. Any product that may be evaluated in this article, or claim that may be made by its manufacturer, is not guaranteed or endorsed by the publisher.

References

Akhoudas, C., Chevalier, N., Blanc-Valleron, M. M., Klein, V., Mendez-Millan, M., Demange, J., et al. (2018). Methane-derived stromatolitic carbonate crust from an active fluid seepage in the Western basin of the sea of marmara: Mineralogical, isotopic and molecular geochemical characterization. *Deep Sea Res. Part II Top. Stud. Oceanogr.* 153, 110–120. doi:10.1016/j.dsr2.2017.12.022

Bangs, N. L. B., Musgrave, R. J., and Trehu, A. M. (2005). Upward shifts in the southern hydrate ridge gas hydrate stability zone following postglacial warming, offshore Oregon. *J. Geophys. Res.* 110, B03102. doi:10.1029/2004jb003293

Blendinger, W. (2004). sea level changes versus hydrothermal diagenesis: Origin of triassic carbonate platform cycles in the dolomites, Italy. *Sediment. Geol.* 178, 141–144. doi:10.1016/j.sedgeo.2005.03.001

Butler, I. B., Bottcher, M. E., Rickard, D., and Oldroyd, A. (2004). Sulfur isotope partitioning during experimental formation of pyrite via the polysulfide and hydrogen sulfide pathways: Implications for the interpretation of sedimentary and hydrothermal pyrite isotope records. *Earth Planet. Sci. Lett.* 228 (3-4), 495–509. doi:10.1016/j.epsl.2004.10.005

Canet, C., Prol-Ledesma, R. M., Escobar-Briones, E., Mortera-Gutiérrez, C., Morales-Puente, P., Linares, C., et al. (2006). Mineralogical and geochemical characterization of hydrocarbon seep sediments from the gulf of Mexico. *Mar. Petroleum Geol.* 23 (5), 605–619. doi:10.1016/j.marpetgeo.2006.05.002

Chazallon, B., Focsa, C., Charlou, J. L., Bourry, C., and Donval, J. P. (2007). A comparative Raman spectroscopic study of natural gas hydrates collected at different geological sites. *Chem. Geol.* 244 (1-2), 175–185. doi:10.1016/j.chemgeo.2007.06.012

Chen, D. F., Dong, F., Zheng, S., Zhi, G. S., Chen, G. Q., and Iii, L. (2006). Pyrite crystallization in seep carbonates at gas vent and hydrate site. *Mater. Sci. Eng. C* 26 (4), 602–605. doi:10.1016/j.msec.2005.08.037

Chown, E. H., N'Dah, E., and Mueller, W. U. (2000). The relation between iron-formation and low temperature hydrothermal alteration in an archean volcanic environment. *Precambrian Res.* 101 (2), 263–275. doi:10.1016/s0301-9268(99)00091-1

Commeau, R. F., Paull, C. K., Commeau, J. A., and Poppe, L. J. (1987). Chemistry and mineralogy of pyrite-enriched sediments at a passive margin sulfide brine seep: Abyssal gulf of Mexico. *Earth Planet. Sci. Lett.* 82 (1-2), 62–74. doi:10.1016/0012-821x(87)90107-5

Cutter, G. A., and Oatts, T. J. (1987). Determination of dissolved sulfide and sedimentary sulfur speciation using gas chromatography-photoionization detection. *Anal. Chem.* 59 (5), 717–721. doi:10.1021/ac00132a008

Egger, M., Rasigraf, O., Sapart, C. J., Jilbert, T., Jetten, M., Roeckmann, T., et al. (2015). Iron-mediated anaerobic oxidation of methane in brackish coastal sediments. *Environ. Sci. Technol.* 49 (1), 277–283. doi:10.1021/es503663z

Fang, Y., Wei, J., Lu, H., Liang, J., Cao, J., Fu, J., et al. (2019). Chemical and structural characteristics of gas hydrates from the haima cold seeps in the qiongdongnan basin of the south China sea. *J. Asian Earth Sci.* 182, 103924. doi:10.1016/j.jseaes.2019.103924

Formolo, M. J., and Lyons, T. W. (2013). Sulfur biogeochemistry of cold seeps in the green canyon region of the gulf of Mexico. *Geochimica Cosmochimica Acta* 119, 264–285. doi:10.1016/j.gca.2013.05.017

Haggerty, J. A. (1991). Evidence from fluid seeps atop serpentine seamounts in the mariana forearc: Clues for emplacement of the seamounts and their relationship to forearc tectonics. *Mar. Geol.* 102 (1-4), 293–309. doi:10.1016/0025-3227(91)90013-t

Hester, K. C., Dunk, R. M., White, S. N., Brewer, P. G., Peltzer, E. T., and Sloan, E. D. (2007). Gas hydrate measurements at hydrate ridge using Raman spectroscopy. *Geochimica Cosmochimica Acta* 71 (12), 2947–2959. doi:10.1016/j.gca.2007.03.032

Hu, Y., Li, H., and Xu, J. (2012). Shallow gas accumulation in a small estuary and its implications: A case history from in and around xiamen bay. *Geophys. Res. Lett.* 39 (24), 2012GL054478. doi:10.1029/2012gl054478

Huang, H., Huang, B., Huang, Y., Li, X., and Tian, H. (2017). Condensate origin and hydrocarbon accumulation mechanism of the deepwater giant gas field in Western south China sea: A case study of lingshui 17-2 gas field in Qiongdongnan basin. *Petroleum Explor. Dev.* 44, 409–417. doi:10.1016/s1876-3804(17)30047-2

Huang, L., Su, Z., and Wu, N. Y. (2015). Evaluation on the gas production potential of different lithological hydrate accumulations in marine environment. *Energy* 91, 782–798. doi:10.1016/j.energy.2015.08.092

Huene, R. V., and Pecher, I. A. (1999). Vertical tectonics and the origins of bsrs along the Peru margin. *Earth Planet. Sci. Lett.* 166 (1-2), 47–55. doi:10.1016/s0012-821x(98)00274-x

Iii, G., and Tsamakis, E. (1989). Concentration and form of dissolved sulfide in the oxic water column of the ocean. *Mar. Chem.* 27 (3-4), 165–177. doi:10.1016/0304-4203(89)90046-7

Jang-Jun, B., Um, I. K., and Holland, M. (2011). Core lithologies and their constraints on gas-hydrate occurrence in the east sea, offshore Korea: Results from the site ubgh1-9. *Mar. Petroleum Geol.* 28 (10), 1943–1952. doi:10.1016/j.marpetgeo.2010.12.003

Kastner, M., Kvenvolden, K. A., and Lorenson, T. D. (1998). Chemistry, isotopic composition, and origin of a methane-hydrogen sulfide hydrate at the cascadia subduction zone. *Earth Planet. Sci. Lett.* 156 (3–4), 173–183. doi:10.1016/s0012-821x(98)00013-2

Kelly, S. L., and Kadish, K. M. (1982). Counterion and solvent effects on the electrode reactions of manganese porphyrins. *Inorg. Chem.* 21, 3631–3639. doi:10.1021/ic00140a010

Kraal, P., Slomp, C. P., Forster, A., Kuypers, M., and Sluijs, A. (2009). Pyrite oxidation during sample storage determines phosphorus fractionation in carbonate-poor anoxic sediments. *Geochimica Cosmochimica Acta* 73 (11), 3277–3290. doi:10.1016/j.gca.2009.02.026

Kump, L. R., Pavlov, A., and Arthur, M. A. (2005). Massive release of hydrogen sulfide to the surface ocean and atmosphere during intervals of oceanic anoxia. *Geol.* 33 (5), 397–400. doi:10.1130/g21295.1

Liang, J., Zhang, W., Lu, J., Wei, J., and He, Y. (2019). Geological occurrence and accumulation mechanism of natural gas hydrates in the eastern Qiongdongnan basin of the South China sea: Insights from site gmgs5-w9-2018. *Mar. Geol.* 418, 106042. doi:10.1016/j.margeo.2019.106042

Lim, Y, C., Lin, S., Yang, T, F., Chen, Y, G., and Liu, C, S. (2011). Variations of methane induced pyrite formation in the accretionary wedge sediments offshore southwestern Taiwan. *Mar. Petroleum Geol.* 28 (10), 1829–1837. doi:10.1016/j.marpetgeo.2011.04.004

Lin, Q., Wang, J. S., Shaoying, F. U., Hongfeng, L. U., Qingtao, B. U., Lin, R. X., et al. (2015). Elemental sulfur in northern south China sea sediments and its significance. *Sci. China Earth Sci.* 58, 2271–2278. doi:10.1007/s11430-015-5182-7

Lin, Q., Wang, J., Taladay, K., Lu, H., Hu, G., Sun, F., et al. (2016). Coupled pyrite concentration and sulfur isotopic insight into the paleo sulfate-methane transition zone (smtz) in the northern south China sea. *J. Asian Earth Sci.* 115, 547–556. doi:10.1016/j.jseaes.2015.11.001

Lin, Z., Sun, X., Strauss, H., Lu, Y., Gong, J., Xu, L., et al. (2017). Multiple sulfur isotope constraints on sulfate-driven anaerobic oxidation of methane: Evidence from authigenic pyrite in seepage areas of the South China sea. *Geochimica Cosmochimica Acta* 211, 153–173. doi:10.1016/j.gca.2017.05.015

Liu, S. W., Lai, Z. P., Wang, Y. X., Fan, X. L., Wang, L. L., Tian, M. Z., et al. (2016). Growing pattern of mega-dunes in the badain jaran desert in China revealed by luminescence ages. *Quat. Int.* 410, 111–118. doi:10.1016/j.quaint.2015.09.048

Liu, X. M., Kah, L. C., Knoll, A. H., Cui, H., Hazen, R. M., Bekker, A., et al. (2021). A persistently low level of atmospheric oxygen in Earth's middle age. *Nat. Commun.* 12 (1), 351. doi:10.1038/s41467-020-20484-7

Mao, S. H., Qin, J. Z., and Li, Y. K. (2021). Re: Mandatory submission of patient identifiable information to third parties: Fgm now, what next? *BMJ* 17 (4), 219–220. doi:10.1136/bmj.h5146

Miao, X., Feng, X., Li, J., and Lin, L. (2021). Tracing the paleo-methane seepage activity over the past 20, 000 years in the sediments of qiongdongnan basin, northwestern south China sea. *Chem. Geol.* 559, 119956. doi:10.1016/j.chemgeo.2020.119956

Millero, F. J., Sotolongo, S., and Izaguirre, M. (1987). Oxidation kinetics of fe(ii) in sea water. *Geochim. Cosmochim. acta* 51, 793–801. doi:10.1016/0016-7037(87)90093-7

Pan, M., Wu, D., Yang, F., Sun, T., Wu, N., and Liu, L. (2018). Geochemical sedimentary evidence from core 973-2 for methane activity near the jiulong methane reef in the northern south China sea. *Interpretation* 6, 1–39. doi:10.1190/INT-2017-0001.1

Peckmann, J., Reimer, A., Luth, U., Luth, C., Reitner, J., Heinicke, C., et al. (2001). Methane-derived carbonates and authigenic pyrite from the northwestern black sea. *Mar. Geol.* 177 (1-2), 129–150. doi:10.1016/s0025-3227(01)00128-1

Peckmann, J., and Thiel, V. (2004). Carbon cycling at ancient methane-seeps. *Chem. Geol.* 205 (3-4), 443–467. doi:10.1016/j.chemgeo.2003.12.025

Qin, J., and Kuhs, W. F. (2013). "Quantitative Raman scattering of guest molecules in gas hydrates and its relevance to gas exchange processes involving N2," in Proceedings of the The Tenth (2013) ISOPE Ocean Mining and Gas Hydrates Symposium, Szczecin, Poland, September 2013.

Qin, X., Liang, Q., Ye, J., Yang, L., Kou, B., Xie, W., et al. (2020). The response of temperature and pressure of hydrate reservoirs in the first gas hydrate production test in south China sea. *Appl. Energy* 278, 115649. doi:10.1016/j.apenergy.2020.115649

Qin, X. W., Zhao, B., Li, F. Y., Zhang, B. J., Wang, H. J., Zhang, R. W., et al. (2019). Deep structure research of the South China sea: Progresses and directions. *China Geol.* 2 (4), 530–540. doi:10.31035/cg2018125

Radford- Knwry, J., and Cutter, G. A. (1994). Biogeochemistry of dissolved hydrogen sulfide species and carbonyl sulfide in the Western north atlantic ocean. *Geochimica Cosmochimica Acta* 58 (24), 5421–5431. doi:10.1016/0016-7037(94)90239-9

Shen, B., Mao, S. H., Kaufman, A. J., Bao, H., Zhou, C., and Wang, H. (2008). Stratification and mixing of a post-glacial Neoproterozoic ocean: Evidence from carbon and sulfur isotopes in a cap dolostone from northwest China. *Earth Planet. Sci. Lett.* 265, 209–228. doi:10.1016/j.epsl.2007.10.005

Shi, Y. H., Liang, Q. Y., Yang, J. P., Yuan, Q. M., Wu, X. M., and Kong, L. (2019). Stability analysis of submarine slopes in the area of the test production of gas hydrate in the south China sea. *China Geol.* 2, 274–284. doi:10.31035/cg2018122

Sima, M., Dold, B., Frei, L., Senila, M., Balteanu, D., and Zobrist, J. (2011). 'Sulfide oxidation and acid mine drainage formation within two active tailings impoundments in the Golden Quadrangle of the Apuseni Mountains, Romania. *J. Hazard. Mater.* 189, 624–639. doi:10.1016/j.jhazmat.2011.01.069

Wan, Z. F., Zhang, W., Ma, C., Liang, J. Q., Li, A., Meng, D. J., et al. (2022). Dissociation of gas hydrates by hydrocarbon migration and accumulation-derived slope failures:an example from the south China sea. *Geosci. Front.* 13 (2), 101345. doi:10.1016/j.gsf.2021.101345

Wang, J., Wu, S., Kong, X., Ma, B., Li, W., Wang, D., et al. (2018a). Subsurface fluid flow at an active cold seep area in the qiongdongnan basin, northern south China sea. *J. Asian Earth Sci.* 168, 17–26. doi:10.1016/j.jseaes.2018.06.001

Wang, J., Wu, S., and Yao, Y. (2018b). Quantifying gas hydrate from microbial methane in the south China sea. *J. Asian Earth Sci.* 168, 48–56. doi:10.1016/j.jseaes.2018.01.020

Wang, S., Magalhães, V. H., Pinheiro, L. M., Liu, J., and Yan, W. (2015). Tracing the composition, fluid source and formation conditions of the methane-derived authigenic carbonates in the gulf of cadiz with rare Earth elements and stable isotopes. *Mar. Petroleum Geol.* 68, 192–205. doi:10.1016/j.marpetgeo.2015.08.022

Wang, X., Liu, B., Jin, J., Lu, J., Zhou, J., Qian, J., et al. (2020). Increasing the accuracy of estimated porosity and saturation for gas hydrate reservoir by integrating geostatistical inversion and lithofacies constraints. *Mar. Petroleum Geol.* 115, 104298. doi:10.1016/j.marpetgeo.2020.104298

Wei, J., Li, J., Wu, T., Zhang, W., Li, J., Wang, J., et al. (2020). Geologically controlled intermittent gas eruption and its impact on bottom water temperature and chemosynthetic communities—a case study in the "HaiMa" cold seeps, south China sea. *Geol. J.* 55 (9), 6066–6078. doi:10.1002/gj.3780

Wu, D., Sun, T., Xie, R., Pan, M., Wu, N., Ye, Y., et al. (2019). Characteristics of authigenic minerals around the sulfate-methane transition zone in the methane-rich sediments of the northern south China sea: Inorganic geochemical evidence. *Int. J. Environ. Res. Public Health* 16 (13), 2299. doi:10.3390/ijerph16132299

Wu, D., Xie, R., Liu, J., Yang, F., Wu, N., Liu, L., et al. (2020). Zone of metal-driven anaerobic oxidation of methane is an important sink for phosphorus in the taixinan basin, south China sea. *Mar. Geol.* 427, 106268. doi:10.1016/j.margeo.2020.106268

Wu, T., Deng, X., Yu, Z., and Wang, L. (2020). Acoustic characteristics of cold-seep methane bubble behavior in the water column and its potential environmental impact. *Acta Oceanol. Sin.* 39 (5), 133–144. doi:10.1007/s13131-019-1489-0

Wu, T., Wei, J., Liu, S., Guan, Y., Zhang, R., Su, M., et al. (2018). Characteristics and formation mechanism of seafloor domes on the north-eastern continental slope of the south China sea. *Geol. J.* 55, 1–10. doi:10.1002/gj.3402

Xie, R., Wu, D., Liu, J., Sun, T., and Wu, N. (2019). Evolution of gas hydrates inventory and anaerobic oxidation of methane (aom) after 40ka in the taixinan basin, south China sea. *Deep Sea Res. Part I Oceanogr. Res. Pap.* 152, 103084. doi:10.1016/j.dsr.2019.103084

Yang, X., Liu, Y., Li, C., Song, Y., Zhu, H., and Jin, X. (2007). Rare Earth elements of aeolian deposits in Northern China and their implications for determining the provenance of dust storms in Beijing. *Geomorphology* 87, 365–377. doi:10.1016/j.geomorph.2006.10.004

Yao, W., and Millero, F. J. (1996). Oxidation of hydrogen sulfide by hydrous fe(iii) oxides in seawater. *Mar. Chem.* 52, 1–16. doi:10.1016/0304-4203(95)00072-0

Yuan, S., Wu, S., Thomas, L., Yao, G., Lv, F., Cao, F., et al. (2009). Fine-grained pleistocene deepwater turbidite channel system on the slope of qiongdongnan basin, northern south China sea. *Mar. Petroleum Geol.* 26 (8), 1441–1451. doi:10.1016/j.marpetgeo.2009.03.007

Zhang, G., Liang, J., Lu, J., Yang, S., Zhang, M., Holland, M., et al. (2015). Geological features, controlling factors and potential prospects of the gas hydrate occurrence in the east part of the pearl river mouth basin, south China sea. *Mar. Petroleum Geol.* 67, 356–367. doi:10.1016/j.marpetgeo.2015.05.021

Zhang, M., Konishi, H., Xu, H., Sun, X., Lu, H., Wu, D., et al. (2014). Morphology and formation mechanism of pyrite induced by the anaerobic oxidation of methane from the continental slope of the ne south China sea. *J. Asian Earth Sci.* 92, 293–301. doi:10.1016/j.jseaes.2014.05.004

Zhang, X. H., Lu, X. B., Chen, X. D., Zhang, L., and Shi, Y. (2016). Mechanism of soil stratum instability induced by hydrate dissociation. *Ocean. Eng.* 122, 74–83. doi:10.1016/j.oceaneng.2016.06.015